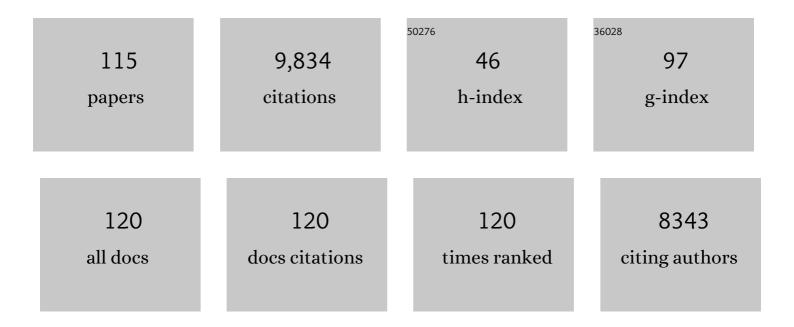
List of Publications by Year in descending order

Source: https://exaly.com/author-pdf/305746/publications.pdf Version: 2024-02-01



HWE REDOMANN

#	Article	IF	CITATIONS
1	High resolution 1s core hole X-ray spectroscopy in 3d transition metal complexes—electronic and structural information. Coordination Chemistry Reviews, 2005, 249, 65-95.	18.8	830
2	X-ray Emission Spectroscopy Evidences a Central Carbon in the Nitrogenase Iron-Molybdenum Cofactor. Science, 2011, 334, 974-977.	12.6	774
3	X-ray damage to the Mn4Ca complex in single crystals of photosystem II: A case study for metalloprotein crystallography. Proceedings of the National Academy of Sciences of the United States of America, 2005, 102, 12047-12052.	7.1	585
4	Structures of the intermediates of Kok's photosynthetic water oxidation clock. Nature, 2018, 563, 421-425.	27.8	386
5	Tracking excited-state charge and spin dynamics in iron coordination complexes. Nature, 2014, 509, 345-348.	27.8	382
6	Simultaneous Femtosecond X-ray Spectroscopy and Diffraction of Photosystem II at Room Temperature. Science, 2013, 340, 491-495.	12.6	378
7	Structure of photosystem II and substrate binding at room temperature. Nature, 2016, 540, 453-457.	27.8	323
8	Absence of Mn-Centered Oxidation in the S2→ S3Transition: Implications for the Mechanism of Photosynthetic Water Oxidation. Journal of the American Chemical Society, 2001, 123, 7804-7820.	13.7	295
9	Probing Valence Orbital Composition with Iron Kβ X-ray Emission Spectroscopy. Journal of the American Chemical Society, 2010, 132, 9715-9727.	13.7	244
10	Taking snapshots of photosynthetic water oxidation using femtosecond X-ray diffraction and spectroscopy. Nature Communications, 2014, 5, 4371.	12.8	206
11	X-ray emission spectroscopy. Photosynthesis Research, 2009, 102, 255-266.	2.9	197
12	The Electronic Structure of Mn in Oxides, Coordination Complexes, and the Oxygen-Evolving Complex of Photosystem II Studied by Resonant Inelastic X-ray Scattering. Journal of the American Chemical Society, 2004, 126, 9946-9959.	13.7	177
13	Nanoflow electrospinning serial femtosecond crystallography. Acta Crystallographica Section D: Biological Crystallography, 2012, 68, 1584-1587.	2.5	167
14	X-ray Absorption Spectroscopy Study of the Hydrogen Bond Network in the Bulk Water of Aqueous Solutions. Journal of Physical Chemistry A, 2005, 109, 5995-6002.	2.5	156
15	Drop-on-demand sample delivery for studying biocatalysts in action at X-ray free-electron lasers. Nature Methods, 2017, 14, 443-449.	19.0	150
16	Untangling the sequence of events during the S ₂ → S ₃ transition in photosystem II and implications for the water oxidation mechanism. Proceedings of the National Academy of Sciences of the United States of America, 2020, 117, 12624-12635.	7.1	149
17	Room temperature femtosecond X-ray diffraction of photosystem II microcrystals. Proceedings of the National Academy of Sciences of the United States of America, 2012, 109, 9721-9726.	7.1	144
18	Accurate macromolecular structures using minimal measurements from X-ray free-electron lasers. Nature Methods, 2014, 11, 545-548.	19.0	140

#	Article	IF	CITATIONS
19	X-ray Emission Spectroscopy To Study Ligand Valence Orbitals in Mn Coordination Complexes. Journal of the American Chemical Society, 2009, 131, 13161-13167.	13.7	135
20	A multi-crystal wavelength dispersive x-ray spectrometer. Review of Scientific Instruments, 2012, 83, 073114.	1.3	130
21	Nearest-neighbor oxygen distances in liquid water and ice observed by x-ray Raman based extended x-ray absorption fine structure. Journal of Chemical Physics, 2007, 127, 174504.	3.0	118
22	Manganese Kβ X-ray Emission Spectroscopy As a Probe of Metal–Ligand Interactions. Inorganic Chemistry, 2011, 50, 8397-8409.	4.0	118
23	Energy-dispersive X-ray emission spectroscopy using an X-ray free-electron laser in a shot-by-shot mode. Proceedings of the National Academy of Sciences of the United States of America, 2012, 109, 19103-19107.	7.1	113
24	Mapping metals in Parkinson's and normal brain using rapid-scanning x-ray fluorescence. Physics in Medicine and Biology, 2009, 54, 651-663.	3.0	112
25	In situ X-ray probing reveals fingerprints of surface platinum oxide. Physical Chemistry Chemical Physics, 2011, 13, 262-266.	2.8	110
26	Metalloprotein entatic control of ligand-metal bonds quantified by ultrafast x-ray spectroscopy. Science, 2017, 356, 1276-1280.	12.6	109
27	1s2p Resonant Inelastic X-ray Scattering of Iron Oxides. Journal of Physical Chemistry B, 2005, 109, 20751-20762.	2.6	108
28	Manipulating charge transfer excited state relaxation and spin crossover in iron coordination complexes with ligand substitution. Chemical Science, 2017, 8, 515-523.	7.4	102
29	X-ray Spectroscopic Observation of an Interstitial Carbide in NifEN-Bound FeMoco Precursor. Journal of the American Chemical Society, 2013, 135, 610-612.	13.7	98
30	Hagfish from the Cretaceous Tethys Sea and a reconciliation of the morphological–molecular conflict in early vertebrate phylogeny. Proceedings of the National Academy of Sciences of the United States of America, 2019, 116, 2146-2151.	7.1	97
31	Site-Selective EXAFS in Mixed-Valence Compounds Using High-Resolution Fluorescence Detection:  A Study of Iron in Prussian Blue. Inorganic Chemistry, 2002, 41, 3121-3127.	4.0	95
32	Mn K-Edge XANES and Kβ XES Studies of Two Mnâ^'Oxo Binuclear Complexes: Investigation of Three Different Oxidation States Relevant to the Oxygen-Evolving Complex of Photosystem II. Journal of the American Chemical Society, 2001, 123, 7031-7039.	13.7	94
33	Observing Solvation Dynamics with Simultaneous Femtosecond X-ray Emission Spectroscopy and X-ray Scattering. Journal of Physical Chemistry B, 2016, 120, 1158-1168.	2.6	85
34	Direct Detection of Oxygen Ligation to the Mn ₄ Ca Cluster of Photosystem II by Xâ€ray Emission Spectroscopy. Angewandte Chemie - International Edition, 2010, 49, 800-803.	13.8	78
35	High-resolution large-acceptance analyzer for x-ray fluorescence and Raman spectroscopy. , 1998, , .		76
36	Metal–Ligand Covalency of Iron Complexes from High-Resolution Resonant Inelastic X-ray Scattering. Journal of the American Chemical Society, 2013, 135, 17121-17134.	13.7	75

#	Article	IF	CITATIONS
37	Structural dynamics in the water and proton channels of photosystem II during the S2 to S3 transition. Nature Communications, 2021, 12, 6531.	12.8	73
38	ldentification of a Single Light Atom within a Multinuclear Metal Cluster Using Valence-to-Core X-ray Emission Spectroscopy. Inorganic Chemistry, 2011, 50, 10709-10717.	4.0	68
39	Chemical Mapping of Paleontological and Archeological Artifacts with Synchrotron X-Rays. Annual Review of Analytical Chemistry, 2012, 5, 361-389.	5.4	64
40	L-Edge X-ray Absorption Spectroscopy of Dilute Systems Relevant to Metalloproteins Using an X-ray Free-Electron Laser. Journal of Physical Chemistry Letters, 2013, 4, 3641-3647.	4.6	64
41	Experimental and Computational X-ray Emission Spectroscopy as a Direct Probe of Protonation States in Oxo-Bridged Mn ^{IV} Dimers Relevant to Redox-Active Metalloproteins. Inorganic Chemistry, 2013, 52, 12915-12922.	4.0	62
42	Probing the oxidation state of transition metal complexes: a case study on how charge and spin densities determine Mn L-edge X-ray absorption energies. Chemical Science, 2018, 9, 6813-6829.	7.4	60
43	Using X-ray free-electron lasers for spectroscopy of molecular catalysts and metalloenzymes. Nature Reviews Physics, 2021, 3, 264-282.	26.6	60
44	The Codex of a Companion of the Prophet and the QurÄn of the Prophet. Arabica, 2010, 57, 343-436.	0.1	57
45	Electronic Structural Changes of Mn in the Oxygen-Evolving Complex of Photosystem II during the Catalytic Cycle. Inorganic Chemistry, 2013, 52, 5642-5644.	4.0	57
46	Synchrotron-based chemical imaging reveals plumage patterns in a 150 million year old early bird. Journal of Analytical Atomic Spectrometry, 2013, 28, 1024.	3.0	55
47	Ultrafast non-radiative dynamics of atomically thin MoSe2. Nature Communications, 2017, 8, 1745.	12.8	52
48	Archimedes brought to light. Physics World, 2007, 20, 39-42.	0.0	49
49	Stimulated X-Ray Emission Spectroscopy in Transition Metal Complexes. Physical Review Letters, 2018, 120, 133203.	7.8	48
50	Synchrotron imaging reveals bone healing and remodelling strategies in extinct and extant vertebrates. Journal of the Royal Society Interface, 2014, 11, 20140277.	3.4	47
51	Localized Electronic Structure of Nitrogenase FeMoco Revealed by Selenium K-Edge High Resolution X-ray Absorption Spectroscopy. Journal of the American Chemical Society, 2019, 141, 13676-13688.	13.7	47
52	High-resolution X-ray spectroscopy of rare events: a different look at local structure and chemistry. Journal of Synchrotron Radiation, 2001, 8, 199-203.	2.4	45
53	Simultaneous detection of electronic structure changes from two elements of a bifunctional catalyst using wavelength-dispersive X-ray emission spectroscopy and in situ electrochemistry. Physical Chemistry Chemical Physics, 2015, 17, 8901-8912.	2.8	45
54	Elemental characterisation of melanin in feathers via synchrotron X-ray imaging and absorption spectroscopy. Scientific Reports, 2016, 6, 34002.	3.3	44

#	Article	IF	CITATIONS
55	Phonon-Suppressed Auger Scattering of Charge Carriers in Defective Two-Dimensional Transition Metal Dichalcogenides. Nano Letters, 2019, 19, 6078-6086.	9.1	43
56	High-resolution structure of the photosynthetic Mn ₄ Ca catalyst from X-ray spectroscopy. Philosophical Transactions of the Royal Society B: Biological Sciences, 2008, 363, 1139-1147.	4.0	42
57	Ligand manipulation of charge transfer excited state relaxation and spin crossover in [Fe(2,2′-bipyridine)2(CN)2]. Structural Dynamics, 2017, 4, 044030.	2.3	41
58	High-Resolution XFEL Structure of the Soluble Methane Monooxygenase Hydroxylase Complex with its Regulatory Component at Ambient Temperature in Two Oxidation States. Journal of the American Chemical Society, 2020, 142, 14249-14266.	13.7	41
59	Structural changes correlated with magnetic spin state isomorphism in the S ₂ state of the Mn ₄ CaO ₅ cluster in the oxygen-evolving complex of photosystem II. Chemical Science, 2016, 7, 5236-5248.	7.4	39
60	X-ray Emission Spectroscopy as an <i>in Situ</i> Diagnostic Tool for X-ray Crystallography of Metalloproteins Using an X-ray Free-Electron Laser. Biochemistry, 2018, 57, 4629-4637.	2.5	39
61	Simultaneous Observation of Carrier-Specific Redistribution and Coherent Lattice Dynamics in 2H-MoTe ₂ with Femtosecond Core-Level Spectroscopy. ACS Nano, 2020, 14, 15829-15840.	14.6	38
62	Electronic Structure of Chemically-Prepared LixMn2O4Determined by Mn X-ray Absorption and Emission Spectroscopies. Journal of Physical Chemistry B, 2000, 104, 9587-9596.	2.6	36
63	Mn oxidation states in tri- and tetra-nuclear Mn compounds structurally relevant to photosystem II: Mn K-edge X-ray absorption and K? X-ray emission spectroscopy studies. Physical Chemistry Chemical Physics, 2004, 6, 4864.	2.8	35
64	Sensitivity of X-ray Core Spectroscopy to Changes in Metal Ligation: A Systematic Study of Low-Coordinate, High-Spin Ferrous Complexes. Inorganic Chemistry, 2013, 52, 6286-6298.	4.0	35
65	Photon-in photon-out hard X-ray spectroscopy at the Linac Coherent Light Source. Journal of Synchrotron Radiation, 2015, 22, 612-620.	2.4	35
66	Carbon speciation in organic fossils using 2D to 3D x-ray Raman multispectral imaging. Science Advances, 2019, 5, eaaw5019.	10.3	35
67	Soft x-ray absorption spectroscopy of metalloproteins and high-valent metal-complexes at room temperature using free-electron lasers. Structural Dynamics, 2017, 4, 054307.	2.3	34
68	Reabsorption of Soft X-Ray Emission at High X-Ray Free-Electron Laser Fluences. Physical Review Letters, 2014, 113, 153002.	7.8	33
69	Electronic Structure of Ni Complexes by X-ray Resonance Raman Spectroscopy (Resonant Inelastic) Tj ETQq1 1 ().784314 ı 13.7	gBT ₃₁ /Overlo
70	Resonant inelastic X-ray scattering (RIXS) spectroscopy at the Mn K absorption pre-edge—a direct probe of the 3d orbitals. Journal of Physics and Chemistry of Solids, 2005, 66, 2163-2167.	4.0	31
71	Generation of High-Power High-Intensity Short X-Ray Free-Electron-Laser Pulses. Physical Review Letters, 2018, 120, 014801.	7.8	31
72	Carrier-Specific Femtosecond XUV Transient Absorption of PbI ₂ Reveals Ultrafast Nonradiative Recombination. Journal of Physical Chemistry C, 2017, 121, 27886-27893.	3.1	30

#	Article	IF	CITATIONS
73	Pheomelanin pigment remnants mapped in fossils of an extinct mammal. Nature Communications, 2019, 10, 2250.	12.8	30
74	Hard X-ray Photon-In Photon-Out Spectroscopy. Synchrotron Radiation News, 2009, 22, 12-16.	0.8	29
75	The mapping and differentiation of biological and environmental elemental signatures in the fossil remains of a 50 million year old bird. Journal of Analytical Atomic Spectrometry, 2015, 30, 627-634.	3.0	28
76	Noninvasive Synchrotron-Based X-ray Raman Scattering Discriminates Carbonaceous Compounds in Ancient and Historical Materials. Analytical Chemistry, 2017, 89, 10819-10826.	6.5	27
77	Optical Control of Non-Equilibrium Phonon Dynamics. Nano Letters, 2019, 19, 4981-4989.	9.1	27
78	Population inversion X-ray laser oscillator. Proceedings of the National Academy of Sciences of the United States of America, 2020, 117, 15511-15516.	7.1	27
79	Structural Investigations of Li[sub 1.5+x]Na[sub 0.5]MnO[sub 2.85]I[sub 0.12] Electrodes by Mn X-Ray Absorption Near Edge Spectroscopy. Journal of the Electrochemical Society, 2000, 147, 395.	2.9	24
80	Complementarity between high-energy photoelectron and L-edge spectroscopy for probing the electronic structure of 5d transition metal catalysts. Physical Chemistry Chemical Physics, 2010, 12, 5694.	2.8	23
81	Methods development for diffraction and spectroscopy studies of metalloenzymes at X-ray free-electron lasers. Philosophical Transactions of the Royal Society B: Biological Sciences, 2014, 369, 20130590.	4.0	23
82	Bacteria or melanosomes? A geochemical analysis of micro-bodies on a tadpole from the Oligocene Enspel Formation of Germany. Palaeobiodiversity and Palaeoenvironments, 2015, 95, 33-45.	1.5	23
83	X-ray free-electron laser studies reveal correlated motion during isopenicillin <i>N</i> synthase catalysis. Science Advances, 2021, 7, .	10.3	23
84	High-Resolution X-ray Emission Spectroscopy of Molybdenum Compounds. Inorganic Chemistry, 2005, 44, 2579-2581.	4.0	22
85	An assessment of multimodal imaging of subsurface text in mummy cartonnage using surrogate papyrus phantoms. Heritage Science, 2018, 6, .	2.3	22
86	Observation of Seeded Mn Kβ Stimulated X-Ray Emission Using Two-Color X-Ray Free-Electron Laser Pulses. Physical Review Letters, 2020, 125, 037404.	7.8	20
87	X-ray absorption spectroscopy using a self-seeded soft X-ray free-electron laser. Optics Express, 2016, 24, 22469.	3.4	19
88	A new synchrotron rapid-scanning X-ray fluorescence (SRS-XRF) imaging station at SSRL beamline 6-2. Journal of Synchrotron Radiation, 2018, 25, 1565-1573.	2.4	19
89	Characterization of charge transfer excitations in hexacyanomanganate(III) with Mn K-edge resonant inelastic x-ray scattering. Journal of Chemical Physics, 2010, 132, 134502.	3.0	18
90	The Mn ₄ Ca photosynthetic water-oxidation catalyst studied by simultaneous X-ray spectroscopy and crystallography using an X-ray free-electron laser. Philosophical Transactions of the Royal Society B: Biological Sciences, 2014, 369, 20130324.	4.0	17

#	Article	IF	CITATIONS
91	Emerging Approaches in Synchrotron Studies of Materials from Cultural and Natural History Collections. Topics in Current Chemistry, 2016, 374, 7.	5.8	17
92	Short-lived metal-centered excited state initiates iron-methionine photodissociation in ferrous cytochrome c. Nature Communications, 2021, 12, 1086.	12.8	17
93	XANES and EXAFS of dilute solutions of transition metals at XFELs. Journal of Synchrotron Radiation, 2019, 26, 1716-1724.	2.4	16
94	Probing a Silent Metal: A Combined X-ray Absorption and Emission Spectroscopic Study of Biologically Relevant Zinc Complexes. Inorganic Chemistry, 2020, 59, 13551-13560.	4.0	16
95	Bioturbating animals control the mobility of redox-sensitive trace elements in organic-rich mudstone. Geology, 2015, 43, 1007-1010.	4.4	14
96	Carrier-specific dynamics in 2H-MoTe2 observed by femtosecond soft x-ray absorption spectroscopy using an x-ray free-electron laser. Structural Dynamics, 2021, 8, 014501.	2.3	14
97	Femtosecond electronic structure response to high intensity XFEL pulses probed by iron X-ray emission spectroscopy. Scientific Reports, 2020, 10, 16837.	3.3	13
98	Double core hole valence-to-core x-ray emission spectroscopy: A theoretical exploration using time-dependent density functional theory. Journal of Chemical Physics, 2019, 151, 144114.	3.0	11
99	Near-Edge X-ray Absorption Fine Structure Spectroscopy of Heteroatomic Core-Hole States as a Probe for Nearly Indistinguishable Chemical Environments. Journal of Physical Chemistry Letters, 2020, 11, 556-561.	4.6	11
100	Pseudo-color enhanced x-ray fluorescence imaging of the Archimedes Palimpsest. Proceedings of SPIE, 2009, , .	0.8	10
101	Effects of x-ray free-electron laser pulse intensity on the Mn K <i>β</i> _{1,3} x-ray emission spectrum in photosystem II—A case study for metalloprotein crystals and solutions. Structural Dynamics, 2021, 8, 064302.	2.3	10
102	Reply to Wang et al.: Clear evidence of binding of Ox to the oxygen-evolving complex of photosystem II is best observed in the omit map. Proceedings of the National Academy of Sciences of the United States of America, 2021, 118, e2102342118.	7.1	7
103	XFEL serial crystallography reveals the room temperature structure of methyl-coenzyme M reductase. Journal of Inorganic Biochemistry, 2022, 230, 111768.	3.5	6
104	Stability of Pt-Modified Cu(111) in the Presence of Oxygen and Its Implication on the Overall Electronic Structure. Journal of Physical Chemistry C, 2013, 117, 16371-16380.	3.1	5
105	Geochemical Evidence of the Seasonality, Affinity and Pigmenation of Solenopora jurassica. PLoS ONE, 2015, 10, e0138305.	2.5	5
106	Decimeter-scale mapping of carbonate-controlled trace element distribution in Neoarchean cuspate stromatolites. Geochimica Et Cosmochimica Acta, 2019, 261, 56-75.	3.9	5
107	A new Devonian euthycarcinoid reveals the use of different respiratory strategies during the marine-to-terrestrial transition in the myriapod lineage. Royal Society Open Science, 2020, 7, 201037.	2.4	5
108	Seasonal calibration of the end-cretaceous Chicxulub impact event. Scientific Reports, 2021, 11, 23704.	3.3	5

#	Article	IF	CITATIONS
109	X-ray Raman Scattering: A Hard X-ray Probe of Complex Organic Systems. Chemical Reviews, 2022, 122, 12977-13005.	47.7	5
110	Photons, Folios, and Fossils: The X-ray Imaging and Spectroscopy Program of Ancient Materials at SSRL. Synchrotron Radiation News, 2019, 32, 22-28.	0.8	4
111	Resonant X-ray emission spectroscopy from broadband stochastic pulses at an X-ray free electron laser. Communications Chemistry, 2021, 4, .	4.5	4
112	Generation of intense phase-stable femtosecond hard X-ray pulse pairs. Proceedings of the National Academy of Sciences of the United States of America, 2022, 119, e2119616119.	7.1	4
113	Disentangling the chemistry of Australian plant exudates from a unique historical collection. Proceedings of the National Academy of Sciences of the United States of America, 2022, 119, .	7.1	4
114	Nouvelles spectroscopies Raman X du carbone pour les matériaux anciens. , 2019, , 22-25.	0.1	1
115	Chemical Mapping of Ancient Artifacts and Fossils with X-Ray Spectroscopy. , 2020, , 2393-2455.		0